Recibido: 22/05/2017
Aceptado: 12/06/2018

REVISTA DE TELEDETECCIÓN
Asociación Española de Teledetección
(2018) 51, 75-85
ISSN 1133-0953
EISSN 1988-8740
https://doi.org/10.4995/raet.2018.7688

Combination of satellite imagery with meteorological data for estimating reference evapotranspiration

Montero, D.*, Echeverry, F., Hernández, F.

Grupo de Investigación en Percepción Remota (GIPER), Universidad del Valle, Calle 13, 100-00, Cali, Colombia.

Abstract: The Food and Agriculture Organization of the United Nations (FAO) in its publication No. 56 of the Irrigation and Drainage Series presents the FAO Penman-Monteith procedure for the estimation of reference evapotranspiration from meteorological data, however, its calculation may be complicated in areas where there are no weather stations. This paper presents an evaluation of the potential of the Land Surface Temperature and Digital Elevation Models products derived from the MODIS and ASTER sensors, both on board the Terra EOS AM-1 satellite, for the estimation of reference evapotranspiration using the Penman-Monteith FAO-56, Hargreaves, Thornthwaite and Blaney-Criddle models. The four models were compared with the method proposed by FAO calculated with the observed data of a ground based meteorological station, finding a significant relation with the models Penman-Monteith FAO-56 and Hargreaves.

Key words: Land Surface Temperature, MODIS, ASTER, reference evapotranspiration, FAO.

Combinación de imágenes satelitales con datos meteorológicos para la estimación de la evapotranspiración de referencia

Resumen: La Organización de las Naciones Unidas para la Alimentación y la Agricultura (FAO) en su publicación No 56 de la Serie de Riego y Drenaje presenta el procedimiento FAO Penman-Monteith para la estimación de la evapotranspiración de referencia a partir de datos meteorológicos, no obstante, su cálculo puede complicarse en zonas donde no se cuenta con estaciones meteorológicas. El presente artículo exhibe una evaluación del potencial de productos de Temperatura Superficial Terrestre y Modelos Digitales de Elevación derivados de imágenes adquiridas por los sensores MODIS y ASTER, ambos a bordo del satélite Terra EOS AM-1, para la estimación de la evapotranspiración de referencia utilizando los modelos de Penman-Monteith FAO-56, Hargreaves, Thornthwaite y Blaney-Criddle. Los cuatro modelos fueron comparados con el método propuesto por la FAO calculado con datos observados de una estación meteorológica en tierra, encontrando una relación significativa con los modelos Penman-Monteith FAO-56 y Hargreaves.

Palabras clave: Temperatura Superficial Terrestre, MODIS, ASTER, evapotranspiración de referencia, FAO.

To cite this article: Montero, D., Echeverry, F., Hernández, F. 2018. Combination of satellite imagery with meteorological data for estimating reference evapotranspiration. *Revista de Teledetección,* 51, 75-85. https://doi.org/10.4995/raet.2018.7688

* *Corresponding author: david.montero@correounivalle.edu.co*

1. Introduction

Evapotranspiration (ET) is an element that links the hydrological cycle and the balance of surface energy, which allows, through the transfer of mass and energy, to maintain propitious water energy levels in the earth-atmosphere system and which is composed of the junction of the transpiration of plants and the evaporation of water present in the soil (Sánchez and Chuvieco, 2000).

Generally, to obtain the ET rate of a crop, expressed in mm per time unit, it is calculated from the surface of a reference grass crop that represents the effect of the climate on the ET process and is known as reference evapotranspiration (ET_o) (Doorenbos and Pruitt, 1977), which is multiplied by a single crop coefficient (K_c) to obtain the ET rate of a specific crop. ET_o is therefore a key component of the hydrological cycle and a basis for estimating the water requirements of a crop (Cruz-Blanco *et al.,* 2014).

Usually, ET_o is obtained by lysimeters, although it can also be obtained from data measured by meteorological stations, using models such as the Penman-Monteith equation FAO-56, Thorntwaite, Linacre, Hargreaves, Kharrufa, Turc, Papdakis, Priestly-Taylor, FAO-Blaney-Criddle or the Radiation Method (Vicente-Serrano *et al.,* 2014), and then it's interpolated or extrapolated according to the case (Manesh *et al.,* 2014), however, extrapolation of ET field data to larger scales is costly, time-consuming and complex because of the heterogeneity of a large-area terrain (Byun *et al.,* 2014).

Since the first launch of meteorological and observational satellites, remote sensing techniques have been considered as possible means to obtain ET information at different spatial and temporal scales (Maselli *et al.,* 2014), hence, ET estimates have great potential for improving the management of water resources in the agricultural sector (Zipper and Loheide, 2014).

This study presents the evaluation of Penman Monteith FAO-56, Hargreaves, Thornthwaite and Blaney-Criddle models for ET_o estimation, calculated in mm d^{-1} on a monthly average scale from the Land Surface Temperature products from MODIS sensor together with supporting data such as the GDEM from ASTER sensor (both sensors on board the Terra EOS AM-1 satellite) and meteorological data obtained by a ground station located in the Cauca river valley, Colombia, where such an estimate could make a methodological contribution in the management of water resources for the irrigation of sugarcane, representative crop of the sector.

2. Materials and methods

2.1. Study area

The study area is located in the Cauca river valley, Valle del Cauca, Colombia (Figure 1), an alluvial plain in the vicinity of the Cauca river at an altitude that varies between 900 and 1100 m. The study area has a tropical savanna climate (Aw) where the rainfall regime has a bimodal distribution with two dry quarters from December to February and from June to August and with two rainy quarters from March to May and from September to November with an average annual precipitation of approximately 1000 mm, an average temperature of 24°C and an average monthly relative humidity that varies between 70 and 75% (Valencia *et al.,* 2017).

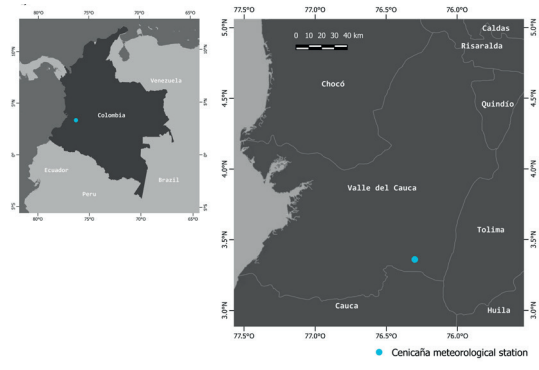

Figure 1. Geographical location of the Cenicaña meteorological station.

2.2. Meteorological data

In this study area, the Sugarcane Research Center of Colombia (Cenicaña), has a network of automated meteorological stations, from which data from the Cenicaña station were used to evaluate the different parameters and models presented here. The station is located on a reference grass

and is equipped with a temperature/humidity sensor (air temperature in °C and relative humidity in percentage units), a pyranometer (solar radiation in cal cm^2 d^{-1}) and an anemometer (wind speed in m s^{-1}). The ET_o calculated with the station data using the Penman-Monteith FAO-56 model was considered as the *in situ* ET_o and was compared to the results obtained by the four ET_o models evaluated in this study.

2.3. Satellite data

Two satellite products were used in this work: The Land Surface Temperature product from the MODIS sensor and the Global Digital Elevation Model from the ASTER sensor. The MODIS (Moderate Resolution Imaging Spectroradiometer) sensor is aboard the Terra EOS AM-1 and Aqua EOS PM-1 satellites, but imagery captured only by the first one was used. These satellites are part of the EOS (Earth Observing System) mission of the National Aeronautics and Space Administration (NASA). Several products derived from the MODIS sensor and its wide range of spectral bands have been developed in order to obtain descriptions of the characteristics of the earth, the ocean and the atmosphere that can be of help for investigative processes at moderate scales. The Land Surface Temperature (LST) data, included in Terra's product MOD11A1, are stored in a 1 km sine grid with the mean daytime and nighttime LST values obtained by the sensor under clear-sky conditions using the MODIS cloud mask product MOD35 (Ackerman *et al.,* 2006), that represent the pixels with potential clouds with no information.

The ASTER (Advanced Spaceborne Thermal Emission and Reflection Radiometer) sensor is aboard the Terra EOS AM-1 satellite and is an instrument developed jointly by the Ministry of Economy, Trade and Industry (METI) of Japan and NASA. The ASTER GDEM Global Digital Elevation Model is developed by Japan Sensor Information Lab Corporation (SILC) thanks to the ability of the ASTER sensor to obtain stereo views in nadir and stern images in the near infrared generating a grid with a 30 m spatial resolution.

2.4. Satellite products preprocessing

The ASTER and MODIS products were reprojected to the WGS84 reference system (EPSG: 4326) using the nearest neighbor algorithm in order to not to alter the original data of each image, adjusting the origins of both products with a 1 km spatial resolution. The LST data of the MOD11A1 product, stored in a 16-bit data type, was transformed to K using the 0.02 conversion factor and then converted to °C. This product, which is found in daily periods, was averaged per month due to the high cloudiness found using a daily periodicity (pixels with no information).

2.5. Baseline parameters

In this study the baseline parameters have been named as all those parameters involved in the calculation of ET_o (Walter *et al.,* 2000; Allen *et al.,* 2006) by the different models used in this study: Penman-Monteith, Hargreaves, Thornthwaite and Blaney-Criddle. The majority of parameters are extracted from satellite instruments, however, some of them can only be obtained from the Cenicaña meteorological station (Table 1).

Table 1. Baseline parameters for the four ET_o models calculation.

Parameter	ET_o model	Formula
Maximum temperature - T_{max} (°C)	Penman-Monteith, Hargreaves	Extracted from MODIS
Minimum temperature - T_{min} (°C)	Penman-Monteith, Hargreaves	Extracted from MODIS
Mean temperature - T_{mean} (°C)	Penman-Monteith, Hargreaves, Thornthwaite, Blaney-Criddle	$T_{mean} = \frac{T_{max} + T_{min}}{2}$
Annual thermal index - I (dimensionless)	Thornthwaite	$I = \sum_{n=1}^{12} (0.2 \times T_{mean})^{1.514}, T_{mean} > 0ºC$
Latitude - ϕ (rad)	Penman-Monteith, Hargreaves, Blaney-Criddle	Extracted from the center of the pixel of MODIS

Table 1 continues in next page

Table 1 continues from previous page

Parameter	ET_o model	Formula
Elevation - z (m)	Penman-Monteith	Extracted from the ASTER GDEM
Atmospheric pressure - P (kPa)	Penman-Monteith	$P = 101.3\left(\frac{293 - 0.0065}{293}\right)^{5.26}$
Psychrometric constant - ɣ (kPa °C^{-1})	Penman-Monteith	$\gamma = \frac{c_p P}{\varepsilon L}$ Where: $c_p = 1.013\times10^{-03}$ MJ kg^{-1} °C^{-1} $\varepsilon = 0.622$ L=2.45MJ kg^{-1}
Saturation vapour pressure - e_s (kPa)	Penman-Monteith	$e_s = \frac{e^o(T_{max}) + e^o(T_{min})}{2}$ Where: $e^o(T) = 0.6108 \times \exp\left[\frac{17.27T}{T + 237.3}\right]$
slope of saturation vapour pressure curve - Δ (kPa °C^{-1})	Penman-Monteith	$\Delta = \frac{4098\left[0.6018 \times \exp\left(\frac{17.27T_{mean}}{T_{mean} + 237.3}\right)\right]}{(T_{mean} + 237.3)^2}$
Actual vapour pressure - e_a (kPa)	Penman-Monteith	For the *in situ* ET_o: $e_a = \frac{e^o(T_{min})\frac{HR_{max}}{100} + e^o(T_{max})\frac{HR_{min}}{100}}{2}$ For the estimated ET_{oPM}: $e_a = e^o(T_{min}) = 0.611\exp\left[\frac{17.27T_{min}}{T_{min} + 237.3}\right]$
Extraterrestrial radiation - R_a (MJ m^{-2} d^{-1})	Penman-Monteith, Hargreaves	$R_a = \frac{24 \times 60}{\pi} G_{sc} d_r [\omega_s \text{sen}(\varphi)\text{sen}(\delta) + + \cos(\varphi)\cos(\delta)\text{sen}(\omega_s)]$ Where: G_{sc}=0.082 MJ m^2 d^{-1} $d_r = 1 + 0.033\cos\left(\frac{2\pi}{365}J\right)$ $\delta = 0.409\,\text{sen}\left(\frac{2\pi}{365}J - 1.39\right)$ $\omega_s = \arccos[-\tan(\varphi)\tan(\delta)]$
Daylight hours - N (h)	Blaney-Criddle	$N = \frac{24}{\pi}\omega_s$
Average daily percentage annual insolation hours - p (%)	Blaney-Criddle	$p = \frac{100N}{\sum_{i=1}^{365} N}$ Where: i=evaluation day
Solar radiation - R_s (MJ m^{-2} d^{-1})	Penman-Monteith	Extracted from the meteorological station
Clear-sky radiation - R_{so} (MJ m^{-2} d^{-1})	Penman-Monteith	$R_{so} = (0.75+2\times10^{-5} z)R_a$
Net shortwave radiation - R_{ns} (MJ m^{-2} d^{-1})	Penman-Monteith	$R_{ns} = (1-\alpha)R_s$

Table 1 continues in next page

Table 1 continues from previous page

Parameter	ET_o model	Formula
Net longwave radiation - R_{nl} (MJ m^{-2} d^{-1})	Penman-Monteith	$R_{nl} = \sigma\left[\frac{T_{max,K}^4 + T_{min,K}^4}{2}\right](0.34 - -0.14\sqrt{e_a})\left(1.35\frac{R_s}{R_{so}} - 0.35\right)$
Net radiation - R_n (MJ m^{-2} d^{-1})	Penman-Monteith	$R_n = R_{ns} - R_{nl}$
Soil heat flux - G (MJ m^{-2} d^{-1})	Penman-Monteith	$G_i = 0.07(T_{mean_{i+1}} - T_{mean_{i-1}})$ Where: i = evaluation month
Wind speed - u_2 (m s^{-1})	Penman-Monteith	Extracted from the meteorological station

The temperature obtained directly from the MODIS product MOD11A1 using the daytime LST as T_{max}, the night LST as T_{min} and the average of both as T_{mean} represent the surface temperature, while the temperature required for the calculation of the ET_o is measured in the air at a height of 2 m. A calibration of the surface temperature obtained directly from the MODIS product was performed using a linear regression between the set of the three temperatures and the set of temperatures measured by the Cenicaña station. The latitude in decimal degrees was obtained by converting one of the temperature images into a latitude raster. The actual vapour pression (e_a) was calculated for the *in situ* ET_o using the relative humidity while for the estimated ET_{oPM} was calculated using an alternative model that involves the T_{min} (Allen *et al.,* 2006) due to the lack of the relative humidity for the satellite imagery calculation.

The remaining parameters were derived from the MODIS temperature, the ASTER elevation, the latitude raster and the combination of parameters obtained from both satellite imagery and the Cenicaña station. Once all parameters were calculated, an evaluation of these parameters was performed by means of the Root Mean Square Error (RMSE) between each of them and their values measured by the Cenicaña meteorological station; the determination coefficient obtained from linear regression analysis was also used for this evaluation.

2.6. Reference evapotranspiration

To estimate ET_o, four evapotranspiration models were used: FAO Penman-Monteith (ET_{oPM}), Hargreaves (ET_{oH}), Thornthwaite (ET_{oT}) and Blaney-Criddle (ET_{oBC}). The Hargreaves, Thornthwaite and Blaney-Criddle models are based on temperatures and latitude, so they can be calculated from data derived only from the MODIS sensor; on the other hand, the Penman-Monteith model is based on other parameters that are obtained from the elevation, the wind speed and the solar radiation, reason why this model is calculated from, besides data derived from the MODIS sensor, data derived from the ASTER sensor and the Cenicaña station measurements.

The ET_{oPM} model is the FAO recommended model (Allen *et al.,* 2006) for the calculation of ET_o in mm d^{-1} and is calculated by equation (1).

$$ET_{oPM} = \frac{0.408\ \ (R_n - G) + \gamma \frac{900}{T_{mean} + 273} u_2 (e_s - e_a)}{+\gamma (1 + 0.34 u_2)} \quad (1)$$

Where Δ is the slope of saturation vapour pressure curve, R_n is the net radiation, G is the soil heat flux, γ is the psychrometric constant, u_2 is the wind speed, e_s is the saturation vapour pressure and e_a is the actual vapour pressure (see Table 1).

The ET_{oH} in mm d^{-1} is the alternative model suggested by FAO (equation 2) in the case that the parameters necessary to calculate the Penman-Monteith model are not available (Hargreaves and Samani, 1982).

$$ET_{oH} = 0.0023 \times R_a (T_{mean} + 17.8)(T_{max} - T_{min})^{0.5} \quad (2)$$

Where R_a must be expressed in mm d^{-1}.

The ET_{oT} model in mm $month^{-1}$ (Thornthwaite, 1948), based on a standard month of 30 days and an average daytime duration of 12 h, is based on the *a* parameter (calculated by equation 3) and the thermal index I (Table 1), to finally calculate the ET_{oT} by equation 4 and convert it to mm d^{-1} by dividing it by the number of days of the month.

$$a = 6.75\times10^{-7} I^3 - 7.71\times10^{-5} I^2 + \\ +1.7912\times10^{-2} I + 0.49239 \quad (3)$$

$$ET_{oT} = 16\left(10\frac{T_{mean}}{I}\right)^a \quad (4)$$

The ET_{oBC} model in mm d^{-1} (Blaney and Criddle, 1950) is another model recommended by FAO for those areas with only temperature and latitude data. This model is calculated by equation 5.

$$ET_{oBC} = p(0.46\times T_{mean} + 8) \quad (5)$$

Where p is the average daily percentage annual insolation hours (Table 1).

The four ET_o models calculated were evaluated by means of linear regression analysis between each of them and the *in situ* ET_o calculated with the data measured by the Cenicaña meteorological station.

3. Results and discussions

Each of the baseline parameters derived from satellite images for the ET_o estimation were compared with the baseline parameters calculated from the data measured by the Cenicaña station and later used for the calculation of the four ET_o models. These results are showed in terms of parameters derived from temperatures, parameters derived from the latitude of the pixel's center, parameters derived from the elevation and the parameters derived from the combination of meteorological data with satellite imagery. After this first comparison, the evaluation of the four ET_o methods is showed.

3.1. Temperature derived from MODIS

The temperatures obtained from the MOD11A1 product were averaged per month since at the coordinates of the Cenicaña station, from which the observed temperature data were obtained, a cloud cover (pixels with no information) was present in 84.8% of daytime LST imagery, 84.7% for nighttime LST imagery and 74.6% for its average (percentages based on a total of 1096 images per set of temperatures). The data of each month were extracted during the study period from the pixel in which the Cenicaña station had its location and a comparison was made between the set of data obtained from MODIS and the data measured by the meteorological station (Figure 2).

Table 2. Statistics of the linear regressions analysis between the MODIS temperatures and the temperature observed by the meteorological station.

	Regression parameters			
Temperature	a	b	R^2	RMSE (°C)
Minimum	18.092	0.051	0.021^{NS}	1.093
Mean	21.834	0.052	0.032^{NS}	1.751
Maximum	22.716	0.229	0.376*	1.879

* Significant at a 99.9% confidence level, ^{NS} Not significant.

It was observed a high variability in MODIS temperatures, which obtained determination coefficients tending to zero and high *p*-values, except for T_{max}, which obtained an R^2 of 0.376 with a *p*-value < 0.0001 (Table 2). However, the errors obtained were relatively small compared to the

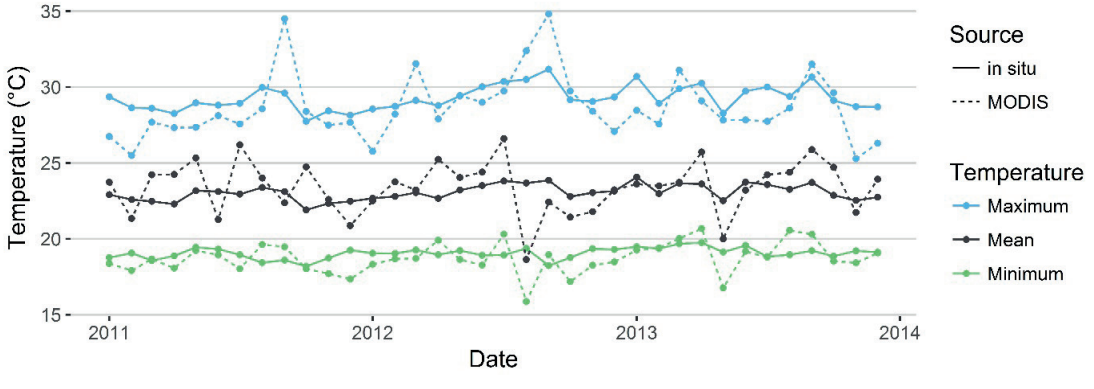

Figure 2. Comparison of the behavior between the air temperature measured by the Cenicaña station (in situ) and the Land Surface Temperature measured by the MODIS sensor.

results obtained by Zhu *et al.* (2013), whose RMSE were 2.97°C for the nighttime LST modeling T_{min} and 7.45°C for the daytime LST modeling T_{max}. It is noteworthy that the RMSE obtained by MODIS temperatures in this study was lower for T_{min} than for T_{mean} or T_{max} as highlighted by different authors (Maeda *et al.,* 2011; Mildrexler *et al.,* 2011).

3.2. Parameters derived from MODIS temperatures

The parameters derived from MODIS Terra temperatures had a high variability (Figure 3) with low determination coefficients and high *p*-values, except for e_s. The annual thermal index I presented an RMSE of 1.871 units compared to the calculated by the temperature measured by the Cenicaña station. The slope of the saturation vapour pressure curve Δ (Figure 3a) and the soil heat flux G (Figure 3d) estimated by the MODIS T_{mean} obtained low determination coefficients ($R^2 < 0.05$; $p > 0.2$) with RMSE values of 0.015 kPa °C^{-1} and 0.155 MJ m^{-2} d^{-1} respectively. The estimated e_a (Figure 3b) was calculated based on the T_{min} of MODIS, while the observed e_a was calculated from relative humidity data measured by the Cenicaña station; this resulted in an R^2 of 0.047 ($p > 0.2$), but the RMSE obtained (0.307 kPa) was similar to the reported by different authors who made the same comparison (Cai *et al.,* 2007, Nolan *et al.,* 2016). The e_s (Figure 3c) obtained a positive relation ($R^2 = 0.372$; $p < 0.0001$) with a RMSE of 0.219 kPa, similar to the reported by Hashimoto *et al.* (2008) when they made the same comparison using MODIS data (0.25 kPa).

3.3. Elevation obtained from the ASTER GDEM version 2

The elevation obtained from the GDEM version 2 of the ASTER sensor showed a difference of 20 m compared to the elevation of the Cenicaña station. In the US, Gesch *et al.* (2012) found an RMSE of 8.68 m, while in Japan Meyer *et al.* (2012) found errors ranging from 6.5 m to 21.7 m with an average of 15.1 m of RMSE, error ranges that cover the 20 m error obtained in the present study. The error in the elevation resulted in an error of 0.219 kPa in the atmospheric pressure and finally an error of 1×10^{-4} kPa °C^{-1} in the psychrometric constant.

3.4. Parameters derived from the latitude of the pixel's center

The parameters derived from the latitude of the pixel's center obtained the best correlations with the same parameters but derived from the latitude

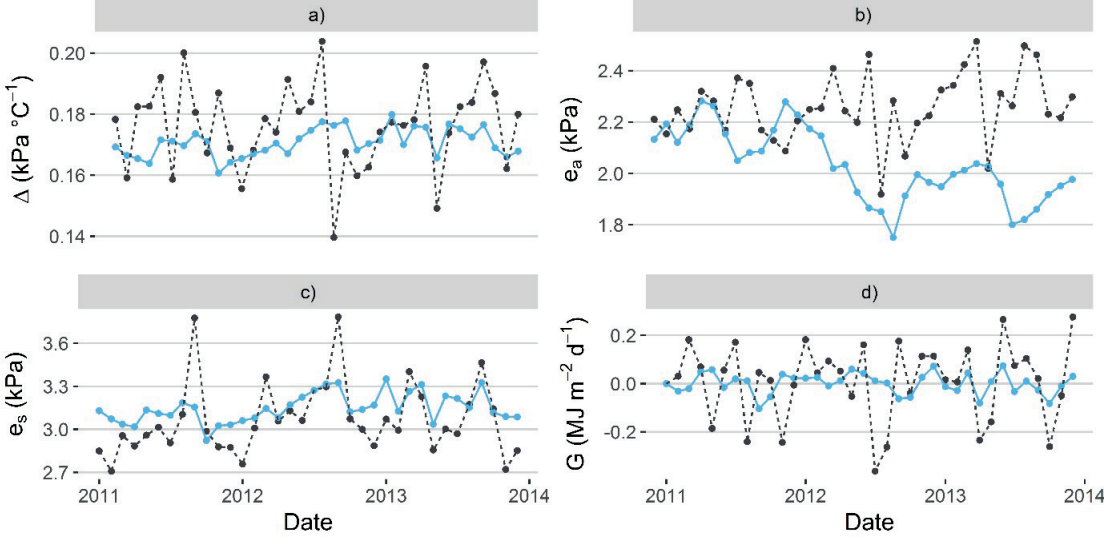

Figure 3. Comparison of the behavior between the parameters derived from the temperature. The continuous blue line represents the parameters calculated by the Cenicaña station data (*in situ*) and the black dotted line represents the parameters calculated by the MODIS sensor.

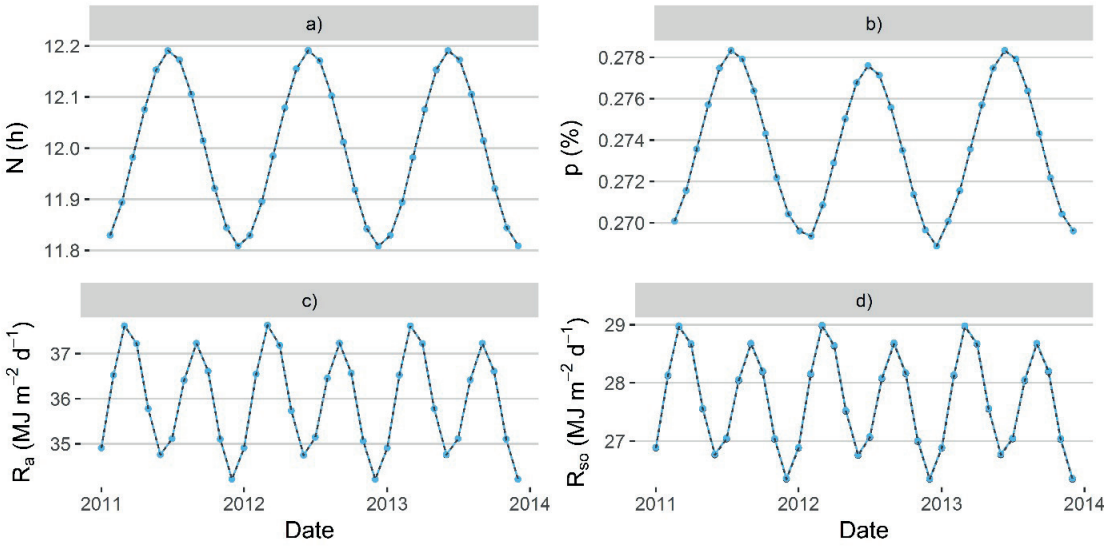

Figure 4. Comparison of the behavior between the parameters derived from the latitude. The continuous blue line represents the parameters calculated by the Cenicaña station data (in situ) and the black dotted line represents the parameters calculated by means of satellite images.

of the Cenicaña station (Figure 4) since moving the latitude only changes the intercept, causing all the parameters to obtain determination coefficients equals to 1 and *p*-values tending to zero. The RMSE obtained by these parameters were the lowest: N (Figure 4a) obtained a RMSE of 6.763×10^{-5} h, p (Figure 4b) obtained a RMSE of 1.543×10^{-6} percentage units, R_a (Figure 4c) only obtained a RMSE of 4.937×10^{-4} MJ m^{-2} d^{-1} and the R_{so} (Figure 4d) obtained an RMSE of 0.014 MJ m^{-2} d^{-1}. These good relations show that the 1 km spatial resolution does not affect greatly the parameters that derive from the latitude of the pixel's center to a distant point that is located in the pixel in question, generating negligible errors for the ET_o calculation.

3.5. Parameters obtained from the combination of images and meteorological data

The parameters that were obtained from combinations of data derived from images and meteorological data showed good results (Figure 5), their errors and lack of precision reflected in the determination coefficients and RMSE were due to the parameters derived from MODIS LST used in the calculation of these new

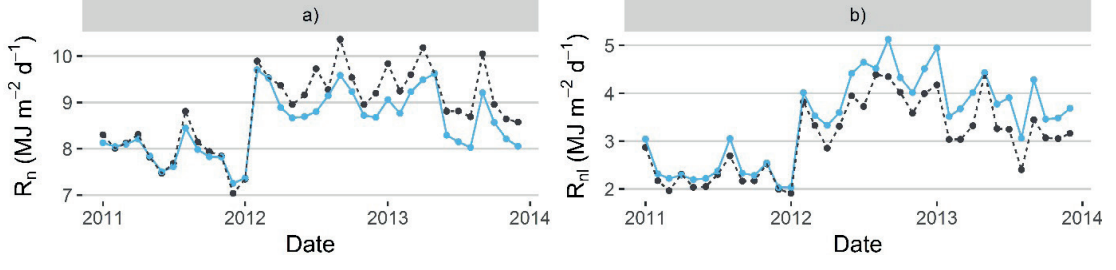

Figure 5. Comparison of the behavior between the parameters obtained from the combination of meteorological data with satellite imagery. The continuous blue line represents the parameters calculated by the Cenicaña station data (in situ) and the black dotted line represents the parameters calculated by means of satellite imagery and its combination with meteorological data.

parameters. In R_{nl} (Figure 5b), the R^2 obtained was equal to 0.935 ($p<0.0001$) with a RMSE of 0.446 MJ m^{-2} d^{-1}, however, tended to underestimate the R_{nl} values calculated by data from the station. Meanwhile, in the calculation of R_n (Figure 5a), the R^2 obtained was equal to 0.904 ($p<0.0001$) with a RMSE of 0.429 MJ m^{-2} d^{-1}, but it overestimated the calculated values of R_n by the station Cenicaña.

3.6. Estimated reference evapotranspiration

Once all the baseline parameters were obtained, the four ET_o models were calculated (Figure 6). The only models that obtained low *p*-values and represented significant relationships with the *in situ* ET_o were the estimated ET_{oPM} ($p<0.0001$) and the estimated ET_{oH} ($p<0.001$). The estimated ET_{oT} and the estimated ET_{oBC} models did not obtain significant relationships (Table 3).

Table 3. Statistics of the linear regressions analysis between the estimated ET_o models and the ET_o observed by the meteorological station.

Model	R^2	RMSE (mm d^{-1})
Penman-Monteith	0.838*	0.214
Hargreaves	0.293*	1.011
Thornthwaite	0.008^{NS}	0.649
Blaney-Criddle	0.009^{NS}	2.004

* Significant at a 99.9% confidence level, ^{NS} Not significant.

The estimated ET_{oPM} was obtained from some parameters that were obtained from different models than the conventional ones for their calculation. The e_a used to calculate the estimated ET_{oPM} was calculated on the basis of the T_{min}, unlike the e_a used for the calculation of the *in situ* ET_o, which was calculated from relative humidity data measured by the Cenicaña station (Allen *et al.,* 2006), which is not available from satellite data. The difference in the calculation of both e_a models finally presented a RMSE between the estimated ET_{oPM} and the *in situ* ET_o. The RMSE in ET_o obtained by Jabloun and Sahli (2008) due to the calculation of the e_a by means of the T_{min} varied between 0.239 and 0.557 mm d^{-1}, whereas the RMSE obtained by Todorovic *et al.* (2013) ranged from 0.360 to 0.680 mm d^{-1} and those obtained by Cai *et al.* (2007) ranged from 0.052 to 0.993 mm d^{-1}; values similar to the RMSE obtained in this study using the same model (RMSE = 0.214 mm d^{-1}). The determination coefficients obtained by these authors in the ET_o models calculated from this e_a were higher than 0.9, however, Sentelhas *et al.* (2010) obtained determination coefficients between 0.76 and 0.96, values that are similar to the determination coefficient for the estimated ET_{oPM} obtained in this study ($R^2=0.838$).

The estimated ET_{oH} obtained a positive relation with the *in situ* ET_o calculated with data from the Cenicaña station, however, this relation was low ($R^2=0.293$) in comparison with the results obtained by other authors, whose coefficients of determination reached values superior to 0.8 (López-Urrea *et al.,* 2006; Jabloun and Sahli, 2008); however, their RMSE reached values up to 0.96 mm d^{-1}, similar to the RMSE value obtained in this study (1.011 mm d^{-1}). The values obtained from the estimated ET_{oH} tended to overestimate the ET_o values in relation to the *in situ* ET_o values, a phenomenon observed by some authors (Berti *et al.,* 2014; Djaman *et al.,* 2015); and that is due, as presented by Martínez-Cob and Tejero-Juste (2004), Gavilán *et al.* (2006) and Cervantes-Osornio *et al.* (2013), to the low wind speed of the study area (approximately 1.5 m s^{-1}), the high

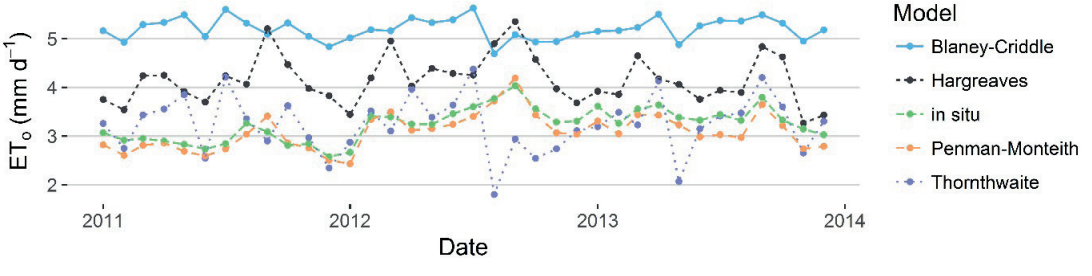

Figure 6. Temporal variation of the estimated ET_o models and the *in situ* ET_o

air humidity (HR_{mean} > 70%) and the location of the study area in non-coastal areas, causing an overestimation of ET_o values and increasing the RMSE in relation to the *in situ* ET_o.

The estimated ET_{oT} obtained a poor accuracy modeling the *in situ* ET_o with a determination coefficient tending to zero ($R^2 = 0.008$), a result similar to the obtained by Vicente-Serrano *et al.* (2014), whose ET_{oT} obtained a null determination coefficient. Nevertheless, the ET_{oT} estimated in this study obtained a relatively small RMSE (RMSE = 0.649 mm d^{-1}) compared to the RMSE obtained by the estimated ET_{oBC} and ET_{oH} (2.004 and 1.011 mm d^{-1} respectively).

The estimated ET_{oBC} overestimated ET_o values in relation to the *in situ* ET_o. It obtained a near zero determination coefficient ($R^2 = 0.009$) and a high RMSE (2.004 mm d^{-1}), values that are compared with those obtained by López- Urrea *et al.* (2006), where ET_{oBC} overestimated ET_o values with RMSE values up to 2.520 mm d^{-1}. Vicente-Serrano *et al.* (2014) obtained ET_{oBC} values that underestimated ET_{oPM} values and, as in the present study, obtained a determination coefficient tending to zero ($R^2 = 0.08$). In contrast, Kashyap and Panda (2001) obtained a R^2 of 0.720 and a RMSE of 0.289 mm d^{-1} whereas Rahimikhoob and Hosseinzadeh (2014) obtained a R^2 of 0.876 modeling the ET_{oPM} from a ET_{oBC} calculated from the NOAA AVHRR land surface temperature data.

4. Conclusions

Although the temperature derived from MODIS did not obtain a very good correlation with the temperature measured by the meteorological station, the error was relatively small and did not generate great errors in the final ET_o.

The parameters involved in the calculation of the ET_o can be effectively derived from satellite imagery data, as well as from its combination with meteorological data. Although some of these parameters do not present a high precision in comparison with the observed data, their low errors do not greatly affect the final ET_o values.

The ET_o estimation is fundamental for the irrigation scheduling of the crops that are present in the study area, especially for the cultivation of sugarcane. The results of this research will allow the agroindustrial sector to know new methodologies for the calculation of the ET_o in order to achieve adequate planning and management of the specific water resources by crop.

Having all the necessary parameters for the calculation of the ET_o with the implementation of satellite and meteorological data, the Penman-Monteith method used in this study turns out to be the most accurate in comparison with its calculation using the conventional methodology that uses the data from the nearest station to a study crop.

If the necessary meteorological parameters recorded by meteorological stations are not available, and only temperature data are available, the Hargreaves method proves to be useful, both derived from satellite imagery and meteorological data, for its simplicity and for its high relation with the data observed in the ET_o estimation by the conventional methodology.

Acknowledgments

The authors thank the Sugarcane Research Center of Colombia (Cenicaña) for providing the necessary data and sharing their knowledge in several of the areas covered here.

References

Ackerman, S., Strabala, K., Menzel, P., Frey, R., Moeller, C., Gumley, L., Baum, B., Seemann, S., Zhang, H. 2006. *Discriminating clear-sky from clouds with MODIS, Algorithm theoretical basis document (MOD35)*. Madison, Wisconsin: University of Wisconsin-Madison.

Allen, R. G., Pereira, L. S., Raes, D., Smith, M. 2006. *Evapotranspiración del cultivo, Guías para la determinación de los requerimientos de agua de los cultivos*. Roma: FAO.

Berti, A., Tardivo, G., Chiaudani, A., Rech, F., Borin, M. 2014. Assessing reference evapotranspiration by the Hargreaves method in north-eastern Italy. *Agricultural Water Management*, 140, 20–25. https://doi.org/10.1016/j.agwat.2014.03.015

Blaney, H. F., Criddle, W. D., 1950. *Determining water requirements in irrigated areas from climatological and irrigation data*. Washington, D.C.: U.S. Soil Conservation Service.

Byun, K., Waqas Liaqat, U., Choi, M. 2014. Dual-model approaches for evapotranspiration analyses over homo and heterogeneous land surface conditions. *Agricultural and Forest Meteorology*, 197, 169–187. https://doi.org/10.1016/j.agrformet.2014.07.001

Cai, J., Liu, Y., Lei, T., Santos Pereira, L. 2007. Estimating reference evapotranspiration with the FAO Penman–Monteith equation using daily weather forecast messages. *Agricultural and Forest Meteorology*, 145, 22–35. https://doi.org/10.1016/j.agrformet.2007.04.012

Cervantes-Osornio, R., Arteaga-Ramírez, R., Vázquez-Peña, M. A., Ojeda-Bustamante, W., Quevedo-Nolasco, A. 2013. Modelos Hargreaves Priestley-Taylor y redes neuronales artificiales en la estimación de la evapotranspiración de referencia. *Ingeniería Investigación y Tecnología*, 14(2), 163-176. https://doi.org/10.1016/S1405-7743(13)72234-0

Cruz-Blanco, M., Gavilán, P., Santos, C., Lorite, I. J. 2014. Assessment of reference evapotranspiration using remote sensing andforecasting tools under semi-arid conditions. *International Journal of Applied Earth Observation and Geoinformation*, 33, 280–289. https://doi.org/10.1016/j.jag.2014.06.008

Djaman, K., Balde, A. B., Sow, A., Muller, B., Irmak, S., N'Diaye, M. K., Manneh, B., Moukoumbi, Y. D., Futakuchi, K., Saito, K. 2015. Evaluation of sixteen reference evapotranspiration methods under sahelian conditions in the Senegal River Valley. *Journal of Hydrology: Regional Studies*, 3, 139–159. https://doi.org/10.1016/j.ejrh.2015.02.002

Doorenbos, J., Pruitt, W. O. 1977. *Guidelines for predicting crop water requirements*. Roma: FAO.

Gavilán, P., Lorite, I. J., Tornero, S., Berengena, J. 2006. Regional calibration of Hargreaves equation for estimating reference ET in a semiarid environment. *Agricultural Water Management*, 81(3), 257–281. https://doi.org/10.1016/j.agwat.2005.05.001

Gesch, D., Oimoen, M., Zhang, Z., Danielson, J., Meyer, D. 2012. Validation of the ASTER Global Digital Elevation Model (GDEM) Version 2 over the Conterminous United States. U.S. In: *International Archives of the Photogrammetry, Remote Sensing and Spatial Information Sciences, Volume XXXIX-B4*. Melbourne, Australia, 15 Agosto – 1 Septiembre. pp 281-286.

Hargreaves, G., Samani, Z. 1982. Estimating potential evapotranspiration. *Journal of the Irrigation and Drainage Division*, 108(3), 225-230.

Hashimoto, H., Dungan, J. L., White, M. A., Yang, F., Michaelis, A. R., Running, S. W., Nemani, R. R. 2008. Satellite-based estimation of surface vapor pressure deficits using MODIS land surface temperature data. *Remote Sensing of Environment*, 112(1), 142–155. https://doi.org/10.1016/j.rse.2007.04.016

Jabloun, M., Sahli, A. 2008. Evaluation of FAO-56 methodology for estimating reference evapotranspiration using limited climatic data Application to Tunisia. *Agricultural Water Management*, 95(6), 707-715. https://doi.org/10.1016/j.agwat.2008.01.009

Kashyap, P. S., Panda, R. K. 2001. Evaluation of evapotranspiration estimation methods and development of crop coefficients for potato crop in a sub-humid region. *Agricultural Water Management*, 50(1), 9-25. https://doi.org/10.1016/S0378-3774(01)00102-0

López-Urrea, R., Martín de Santa Olalla, F., Fabeiro, C., Moratalla, A. 2006. Testing evapotranspiration equations using lysimeter observations in a semiarid climate. *Agricultural Water Management*, 85, 15-26. https://doi.org/10.1016/j.agwat.2006.03.014

Maeda, E. E., Wiberg, D. A., Pellikka, P. K. E. 2011. Estimating reference evapotranspiration using remote sensing and empirical models in a region with limited ground data availability in Kenya. *Applied Geography*, 31, 251-258. https://doi.org/10.1016/j.apgeog.2010.05.011

Manesh, S. S., Ahani, H., Rezaeian-Zadeh, M. 2014. ANN-based mapping of monthly reference crop evapotranspiration by using altitude, latitude and longitude data in Fars province, Iran. *Environment, Development and Sustainability*, 16(1), 103–122. https://doi.org/10.1007/s10668-013-9465-x

Martínez-Cob, A., Tejero-Juste, M. 2004. A wind-based qualitative calibration of the Hargreaves ET_0 estimation equation in semiarid regions. *Agricultural Water Management*, 64(3), 251–264. https://doi.org/10.1016/S0378-3774(03)00199-9

Maselli, F., Papale, D., Chiesi, M., Matteucci, G., Angeli, L., Raschi, A., Seufert, G. 2014. Operational monitoring of daily evapotranspiration by the combination of MODIS NDVI and ground meteorological data: Application and evaluation in Central Italy. *Remote Sensing of Environment*, 152, 279–290. https://doi.org/10.1016/j.rse.2014.06.021

Meyer, D. J., Tachikawa, T., Abrams, M., Crippen, R., Krieger, T., Gesch, D., Carabajal, C. 2012. Summary of the validation of the second version of the ASTER GDEM. In: *International Archives of the Photogrammetry, Remote Sensing and Spatial Information Sciences, Volume XXXIX-B4.* Melbourne, Australia, 15th August – 1st September. pp 291-293. https://doi.org/10.5194/isprsarchives-XXXIX-B4-291-2012

Mildrexler, D. J., Zhao, M., Running, S. W. 2011. A global comparison between station air temperatures and MODIS land surface temperatures reveals the cooling role of forests. *Journal Of Geophysical Research*, 116, 1-15. https://doi.org/10.1029/2010JG001486

Nolan, R. H., Resco de Dios, V., Boer, M. M., Caccamo, G., Goulden, M. L., Bradstock, R. A. 2016. Predicting dead fine fuel moisture at regional scales using vapour pressure deficit from MODIS and gridded weather data. *Remote Sensing of Environment*, 174, 100–108. https://doi.org/10.1016/j.rse.2015.12.010

Rahimikhoob, A., Hosseinzadeh, M. 2014. Assessment of Blaney-Criddle Equation for Calculating Reference Evapotranspiration with NOAA/AVHRR Data. *Water Resour Manage*, 28(10), 3365–3375. https://doi.org/10.1007/s11269-014-0670-7

Sánchez, M., Chuvieco, E. 2000. Estimación de evapotranspiración del cultivo de referencia, ET_o, a partir de imágenes NOAA-AVHRR. *Revista de Teledetección*, 14, 1-10. Available at: http://www.aet.org.es/?q=revista14-2 [Last access: June 2018].

Sentelhas, P. C., Gillespie, T. J., Santos, E. A. 2010. Evaluation of FAO Penman–Monteith and alternative methods for estimating reference evapotranspiration with missing data in Southern Ontario, Canada. *Agricultural Water Management*, 97(5), 635–644. https://doi.org/10.1016/j.agwat.2009.12.001

Thornthwaite, C. W. 1948. An Approach toward a Rational Classification of Climate. *Geographical Review*, 38(1), 55-94. https://doi.org/10.2307/210739

Todorovic, M., Karic, B., Pereira, L. S. 2013. Reference evapotranspiration estimate with limited weather data across a range of Mediterranean climates. *Journal of Hydrology*, 481, 166–176. https://doi.org/10.1016/j.jhydrol.2012.12.034

Valencia, J. M., García, C. E., Montero, D. 2017. Anomalías de vegetación asociadas con el fenómeno del ENOS en el valle geográfico del río Cauca, Colombia. *Revista de Teledetección*, 50, 89-99. https://doi.org/10.4995/raet.2017.7715

Vicente-Serrano, S. M., Azorin-Molina, C., Sanchez-Lorenzo, A., Revuelto, J., López-Moreno, J. I., González-Hidalgo, J. C., Morán-Tejadam E., Espejo, F. 2014. Reference evapotranspiration variability and trends in Spain, 1961–2011. *Global and Planetary Change*, 121, 26–40. https://doi.org/10.1016/j.gloplacha.2014.06.005

Walter, I. A., Allen, R. G., Elliott, R., Jensen, M., Itenfisu, D., Mecham, B., Howell, T., Snyder, R., Brown, P., Echings, S., Spofford, T., Hattendorf, M., Cuenca, R. H., Wright, J. L., Martin, D. 2000. ASCE Standarized Reference Evapotranspiration Equation. In: *Watershed Management and Operations Management 2000*. Fort Collins, Colorado, U.S., june 20-24. pp 1-11.

Zipper, S. C., Loheide, S. P. 2014. Using evapotranspiration to assess drought sensitivity on a subfield scale with HRMET, a high resolution surface energy balance model. *Agricultural and Forest Meteorology*, 197, 91–102. https://doi.org/10.1016/j.agrformet.2014.06.009

Zhu, W., Lü, A., Jia, S. 2013. Estimation of daily maximum and minimum air temperature using MODIS land surface temperature products. *Remote Sensing of Environment*, 130, 62–73. https://doi.org/10.1016/j.rse.2012.10.034